

Documentation of Updates to the PAGE-2020 Model

James Rising*

June 1, 2025

1 Description of Updates

Prior to this paper, the PAGE model included eight multi-country regions. Table 1 summarizes the updates to the PAGE-2020 model in this paper, associated with improvements in the spatial resolution of the model.

Improvement	Description
Country-level regions	Baseline data describing 183 countries or country aggregates, following <i>de facto</i> borders
Extension of the SSPs	National population and GDP projections projected to 2300
RFF Probabilistic Projections	Modeling using the RFFSPs, as used by the U.S. EPA SCC process
Climate downscaling	ESM-based pattern downscaling, using a probabilistic mapping between global temperatures and ESM patterns
International spill-overs	Estimation of supply chain impacts using a global input-output model
Market damages	Empirically-calibrated country-level differential vulnerability, indexed to the INFORM risk characteristics
Non-market damages	Improved country-level non-market damages based on meta-analysis and equations from the MERGE model
Sea-level rise damages	Emulation of country-level SLR and storm surge damages under different adaptation scenarios from pyCIAM
Abatement costs	Emulation of country-level abatement cost curves based on NGFS energy model downscaling
Downscaled CO ₂ and CH ₄	Country-level emissions for CO ₂ and CH ₄
Subnational damages	Using correlated distributions of income and vulnerability, we calculate correction factors for national and global SCCs.

Table 1: Improvements correspond to sections below.

1.1 Country-level Regions

There is considerable disagreement across national and international institutions concerning the number of sovereign countries, and their boundaries and income measures. We have tried to develop an appropriate account of countries, with the following datasets:

Population drawn from the UN World Population Prospects (<https://population.un.org/wpp/>)

Gross Domestic Product from the World Bank in current USD for 2015 (<https://data.worldbank.org/indicator/NY.GDP.MKTP.PP.CD>)

*jrising@udel.edu

Boundaries from Natural Earth, which uses *de facto boundaries*. <https://www.naturalearthdata.com/>.

Temperatures from the ECMWF ERA5 Reanalysis (<https://www.ecmwf.int/en/forecasts/dataset/ecmwf-reanalysis-v5>).

Some smaller regions are missing from some datasets, and these gaps are filled in from multiple sources.

All countries with populations greater than 300 thousand (2015 estimate) are included individually, and the remaining have been grouped into five aggregates (see figure 1). The country-level version of PAGE includes 178 countries and 5 additional aggregate regions.

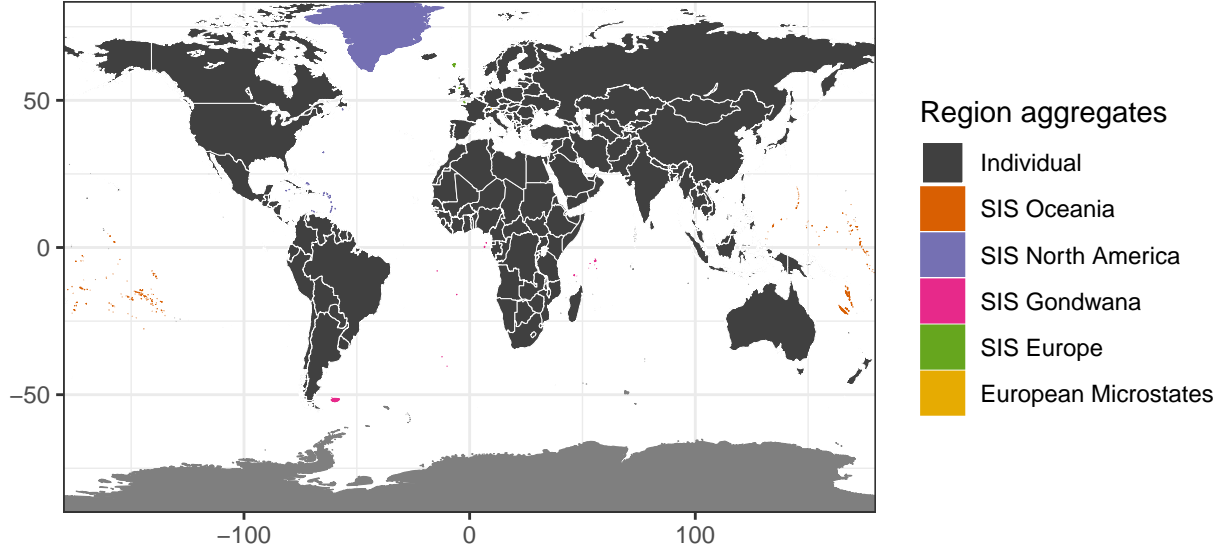


Figure 1: Regions to be used in the country-level PAGE model.

1.2 Extension of the SSPs

The following text is modified from the supplemental information descriptions in Dietz et al. [2021] and Kikstra et al. [2021]. The associated code is in <https://github.com/openmodels/SSP-Extensions>.

To estimate population and income levels past 2100 along the Shared Socioeconomic Pathways (SSP) scenarios, we fit a model to the available pre-2100 SSP scenario data and use the fitted model to extrapolate. The same model is applied to both income and population and is defined in terms of growth rates. The model postulates that changes in pre-2100 income and population growth rates are explained by a rate of convergence and a rate of decay.

The model is as follows:

$$\text{Growth}_{it} = (1 - \beta - \delta)\text{Growth}_{i,t-1} + \delta\text{MeanGrowth}_{t-1}, \quad (1)$$

where i indexes the region, t indexes years, δ is the rate of convergence, β is the decay rate and

$$\text{MeanGrowth}_{t-1} = \sum_i \frac{\text{Population}_{i,2015}}{\sum_j \text{Population}_{j,2015}} \text{Growth}_{i,t-1}. \quad (2)$$

Below, we write this as $\text{Growth}_{\cdot,t-1} \cdot w$, where w is the vector of global population shares for each country.

Region	Region Code	Population 2015 (in million)	GDP 2015 for million 2015 US \$)	Land Area (Sq. Km)	Marine Area (Sq. Km)	Baseline Land Temp (C)
United States of America	USA	325	18206021	9464228	6142456	8.1
China	CHN	1394	11061573	9375239	1302395	6.9
Japan	JPN	127	4444931	373508	4068137	12.0
Germany	DEU	82	3357586	357674	56763	9.7
United Kingdom	GBR	65	2934858	243783	739320	9.4
France	FRA	66	2439189	636759	1435758	13.1
India	IND	1323	2103588	3150747	2323935	23.8
Italy	ITA	60	1836638	301185	536654	12.9
Brazil	BRA	205	1802212	8472670	3677664	25.2
Canada	CAN	36	1556509	9945630	5765316	-5.4
Republic of Korea	KOR	51	1465773	98544	430281	12.4
Russian Federation	RUS	145	1363482	16980200	7734809	-4.2
Australia	AUS	24	1350580	7691175	7347269	22.2
Spain	ESP	46	1196157	506884	561789	14.2
Mexico	MEX	120	1171870	1957847	3187013	21.0
Türkiye	TUR	80	864314	780080	262233	12.2
Indonesia	IDN	259	860854	1879827	6020917	25.4
Netherlands	NLD	17	765573	37398	64328	10.7
Switzerland	CHE	8	694118	41436	0	6.7
Saudi Arabia	SAU	33	669484	1921725	224219	26.4
Small Islands - North America	SIS-NAmer	1620	37116	2160087	3645009	23.1
Small Islands - Europe	SIS-Europe	364	25041	2119	276350	12.1
Small Islands - Oceania	SIS-Oceania	1780	24634	42035	21740928	26.3
European Microstates	EUR-Micro	143	10478	650	0	9.5
Small Islands - South America,	SIS-Gondwana	309	1741	13437	3710836	19.4
Africa, and Around						

Table 2: Basic statistics for top 20 economies (by GDP) and the aggregate regions.

SSP data are not available in every year, so fitting Eq. (1) requires a model with dynamics. We use a two-step approach, fitting the model using Stan, a computational Bayes system. The first step uses the available data directly, fitting

$$\text{Growth}_{is} \sim \mathcal{N}([1 - \Delta t(\beta + \delta)]\text{Growth}_{i,s-1} + \Delta t\delta\text{MeanGrowth}_{s-1}, \sigma_i), \quad (3)$$

where s is a time step, Δt is the number of years between time steps, and country i has uncertainty σ_i . We apply a prior that both β and δ are between 0 and 0.5.

Next, we fit the full model, using the results of the simplified model to improve the Bayesian model convergence. In this case, for a given Markov chain Monte Carlo draw of β and δ , we calculate the entire time series:

$$\widehat{\text{Growth}}_{it} \sim \mathcal{N}\left((1 - \beta - \delta)\widehat{\text{Growth}}_{i,t-1} + \delta \left[\widehat{\text{Growth}}_{.,t-1} \cdot w.\right], \sigma_i\right) \quad (4)$$

starting with $\widehat{\text{Growth}}_{i,2015}$ as reported in the SSP dataset.

The probability evaluation is over both the performance of the fit and the priors:

$$\begin{aligned} \text{Growth}_{is} &\sim \mathcal{N}\left(\widehat{\text{Growth}}_{i,t(s)}, \sigma_i\right) \\ \beta &\sim \mathcal{N}(\mu_\beta, \sigma_\beta) \\ \delta &\sim \mathcal{N}(\mu_\delta, \sigma_\delta) \\ \log \sigma_i &\sim \mathcal{N}(\mu_{\sigma,i}, \sigma_{\sigma,i}) \end{aligned}$$

where $\mu.$ is the mean estimate for the corresponding parameter, and $\sigma.$ is the standard deviation across its uncertainty. The prior for σ_i is defined as a log-normal, centered on the mean of the estimates of $\log \sigma_i$.

The estimates for each SSP are shown in Table 3, with visualizations of timeseries data for SSP2 and SSP5 in Figure 2.

Extrapolated global population

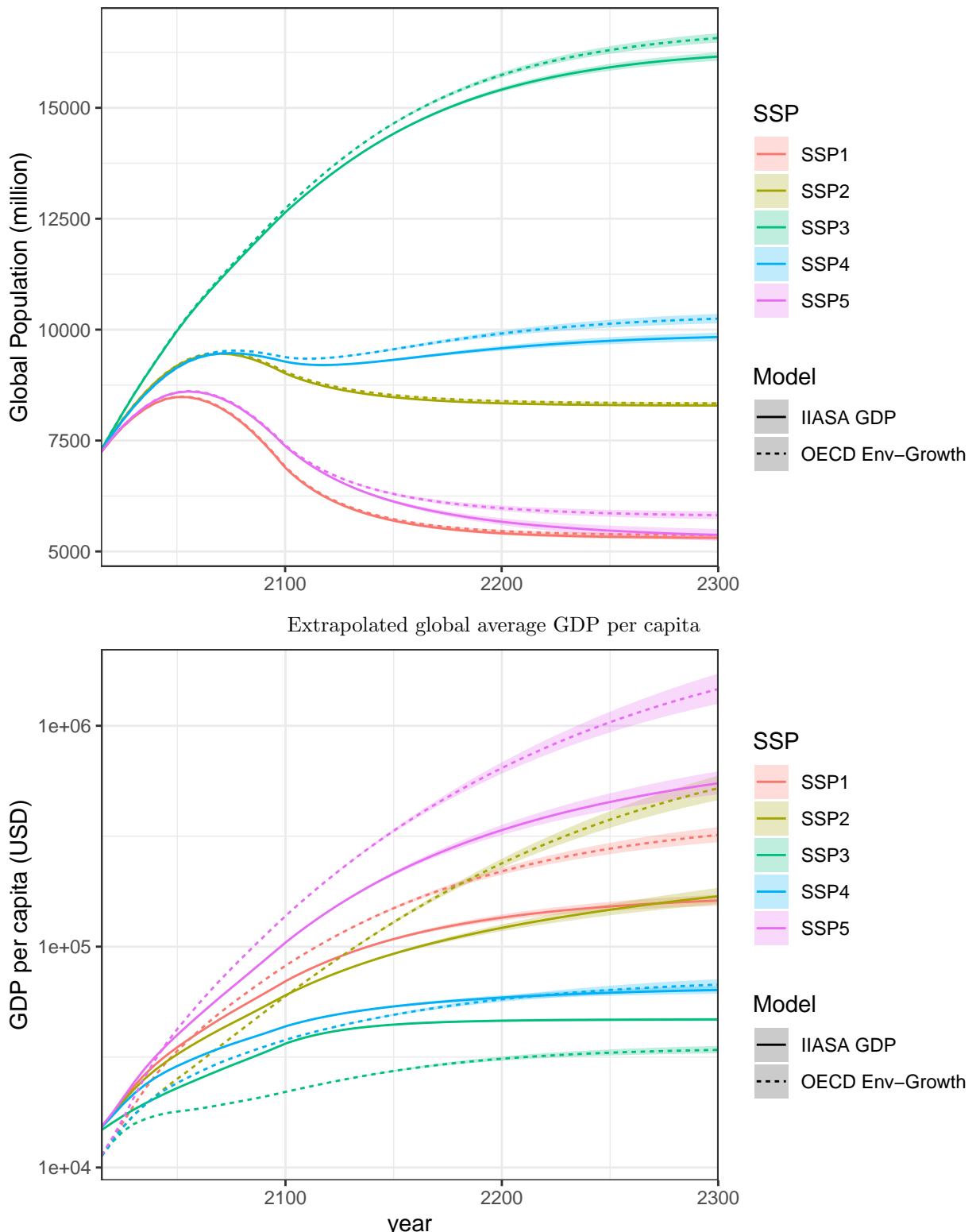


Figure 2: Extended SSP population and GDP per capita by SSP and model. Shaded areas show 95% credible intervals. Both macroeconomic models used to calculate the SSPs are shown.

SSP	Variable	δ	β
1	GDP per capita	0.006205028	0.005930520
1	Population	0.008967453	0.005215835
2	GDP per capita	0.004190444	0.007228942
2	Population	0.001276993	0.011064426
3	GDP per capita	0.006273030	0.009597363
3	Population	0.001064697	0.007688331
4	GDP per capita	0.006895296	0.009651277
4	Population	0.001867587	0.003461600
5	GDP per capita	0.007766807	0.003843256
5	Population	0.003470952	0.004305310

Table 3: Estimated convergence and decay rates for extrapolation of growth of GDP per capita and population in the SSP socio-economic scenarios beyond 2100

1.3 RFF Probabilistic Scenarios

We further allow the probabilistic scenario and baseline emissions from the RFF probabilistic scenarios [Rennert et al., 2022b]. In particular, we rely upon the Monte Carlo estimates of population growth and GDP per capita growth by country. We also use these to adjust the emissions growth rates, following a simplified Kaya identity: Emissions = (Population)(GDP per capita)(Emissions Intensity of GDP). Assuming that the emissions intensity of GDP is unchanged for a given country and time period, we can adjust the emissions from the SSPs as follows:

$$\text{Emissions} = \text{Emissions}_{\text{SSP}} \text{GDP}_{\text{RFF}} / \text{GDP}_{\text{SSP}}$$

which implies that

$$\text{Emissions growth} = \text{Emissions growth}_{\text{SSP}} + \text{GDP growth}_{\text{RFF}} + \text{GDP growth}_{\text{SSP}}$$

1.4 Climate Downscaling

We apply an improved Monte Carlo pattern/residual (MCPR) method to map simple climate model GMST temperatures to country-level temperature patterns [Rasmussen et al., 2016]. The method used by Rasmussen et al. [2016] decomposes GCM warming into a global component and residual patterns, and then patterns can be applied randomly. Instead of using patterns across the entire temperature range, we assign patterns to different overlapping segments of the temperature space, like the surrogate/model mixed ensemble (SMME) method described by the same reference.

We use a collection of downscaled GCMs from Fick and Hijmans [2017] (WorldClim) to represent the variation in patterns of warming across the globe. Each warming pattern is applied to the global mean warming levels given by the PAGE Monte Carlo runs. The WorldClim downscaled results are available for 9 GCMs, at 10” resolution, as 20-year averages.

The comparison to the global GCM warming levels to the distribution from FaIR (similar to PAGE’s climate model) is shown in figure 3.

To assign a GCM warming pattern to each FaIR Monte Carlo scenario, we start by determining the reliability of ordering between the GCM models. If the GCMs had identical warming patterns, the order of GCMs according to global temperatures would match the order of GCMs for each pixel. In this case, we would strictly partition the temperature space, assigning a range of temperatures to each GCM. If there

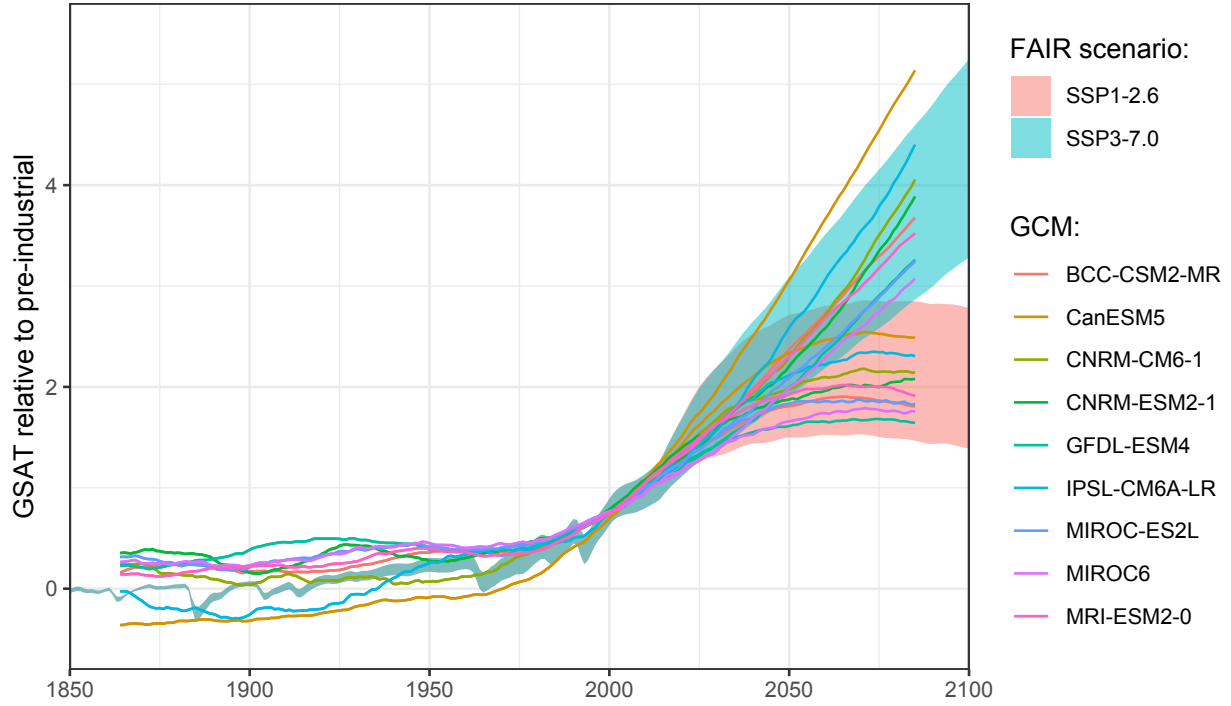


Figure 3: The confidence intervals around FaIR Monte Carlos, compared to the downscaled GCMs.

is disagreement between the ordering of GCMs at a pixel level, the warming ranges for each GCM should correspondingly overlap.

We define the relative probability of each GCM at a given temperature level according to a normal distribution. The temperature in 2081-2100 is taken as an index of the warming for each model. The relative probability of GCM i at 2081-2100 temperature T is $N(T|T_{GCM}, \tau)$. τ determines the degree of overlap between models.

To determine the degree of overlap, we calculate grid-level correlations between GCM-anomalies and GCM-level temperature. We then calibrate τ so that the correlation between the vector of 2081-2100 global temperatures and the temperatures for the stochastically assigned GCMs matches this correlation. We find that $\tau = 0.2158$ for SSP1-2.6, and $\tau = 0.4013$ for SSP3-7.0. We then determine a pattern for each hundredth of a degree in 2100 which is identical for both SSP scenarios, by randomly drawing GCMs using this method for each Monte Carlo until both scenarios give the same pattern. The final assignment of patterns is shown in figure 4.

1.5 International Trade

The international trade module estimates how much of each country's GDP is lost due to climate impacts on that country's trading partners. While a Computable General Equilibrium (CGE) approach would be most comprehensive, the macro-level of damages in PAGE motivates an alternative approach. We use the Eora26 Multi-Region Input-Output tables in 2015 and UN ComTrade imports and exports to calculate these losses, based on a method that disaggregates global losses based on Domar weights ?.

The Eora26 MRIO transaction matrix for 2015 is aggregated nationally by summing within each 26x26 industry block, and summing across columns of the value added and final demand matrices. We then calculate total sales as the row sums of the transaction matrix plus the final demands, and GDP as the value

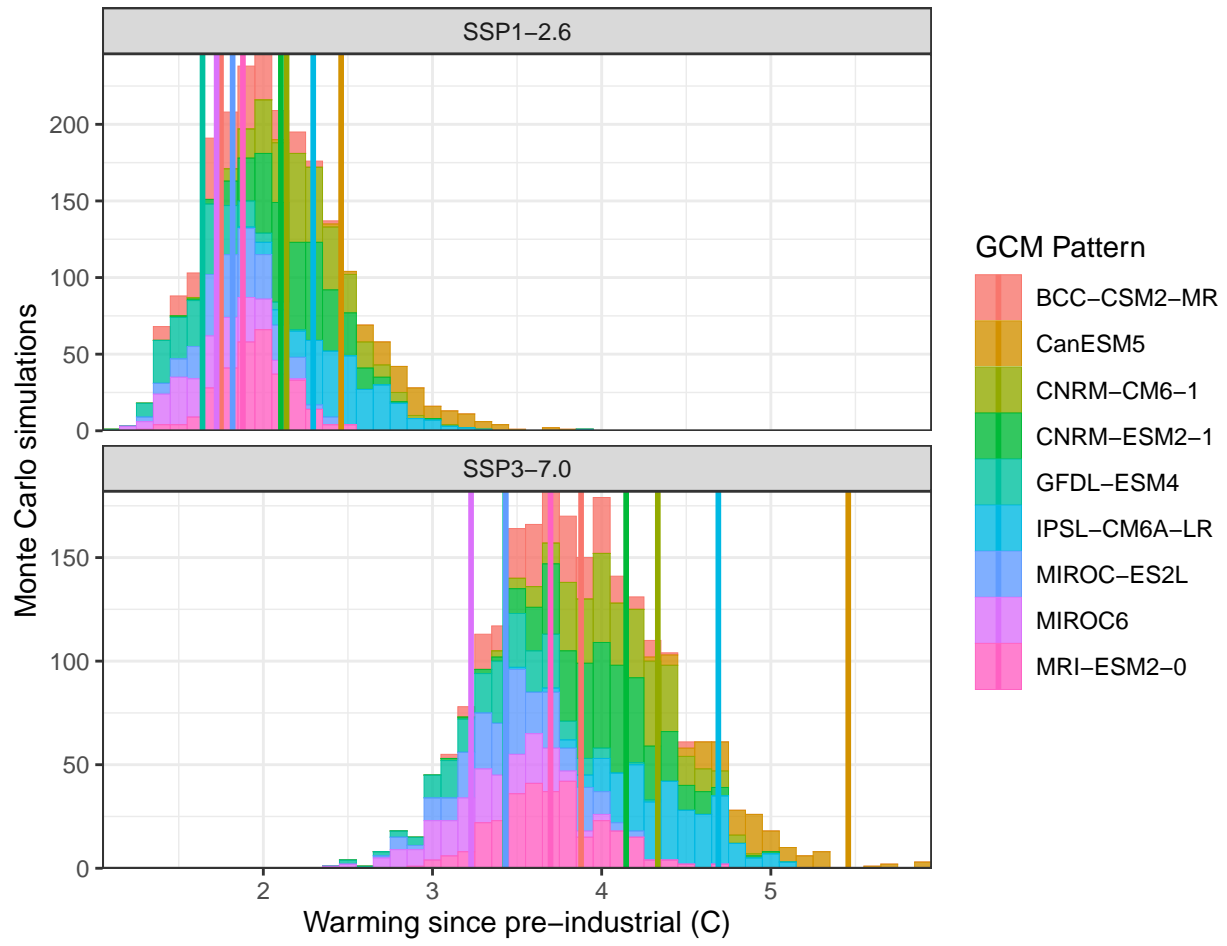


Figure 4: The assigned patterns for each Monte Carlo run of FaIR.

added plus the final demand. The total global impact, accounting for spill-overs, is then

$$GlobalImpact_t = \sum_i TotalSales_{it} LocalImpact_{it} / \sum_i GDP_{it}$$

The additional spill-over effect is then

$$TradeImpact_t = GlobalImpact_t - \sum_i LocalImpact_{it} GDP_{it} / \sum_i GDP_{it}$$

In each year, we also calculate the Free on board export value lost, assuming a direct relationship between losses in country j and its exports to all other countries,

$$ExportLoss_{it} = \sum_j FOBValue_{ijt} LocalImpact_{it} / \sum_j FOBValue_{ijt}$$

To understand the relationship between trade and GDP under CGE modeling, we use Brexit CGE studies to calibrate the international effect of impacts operating through the international trade network on the United Kingdom. The Brexit CGE results that form the basis of this relationship are shown in Table 4, and the empirical relationship between import and export changes to GDP loss is shown in Table 5.

Source	Scenario	% GDP	% Exports	% Imports	Method
Latorre et al. 2019	Soft (Norway case)	-1.23	-7.54	-6.44	GAMS
Latorre et al. 2019	Hard (WTO case)	-2.53	-16.94	-14.42	GAMS
Dhingra et al. 2017	Soft Brexit scenario	-1.34	-9.00	-14.00	Eaton–Kortum
Dhingra et al. 2017	Hard Brexit scenario	-2.66	-16.00	-16.00	Eaton–Kortum

Table 4: Estimated losses to GDP, imports, and exports from selected Brexit studies. .

<i>Dependent variable:</i>	
% GDP	
% Exports	0.160** (0.027)
% Imports	-0.003 (0.027)
Observations	4
R ²	0.997
Adjusted R ²	0.995
Residual Std. Error	0.151 (df = 2)
F Statistic	364.835*** (df = 2; 2)

Note: *p<0.1; **p<0.05; ***p<0.01

Table 5: Regression table based on the observations in Table 4.

We see that changes in exports are a strong predictor for changes in GDP. We assume that exports from a trading partner are reduced by the same fraction as the GDP, and look for a common value (in place of the 0.16 from table 5) that allows these impacts to be consistent with the Domar weights value, so that the sum of $ExportLoss_{it}$ equals the $TradeImpact_t$.

This value can be noisy, so we take the average scaling value over the years prior to and including year t , and apply this $ExportLoss_{it}$ to get the trade loss.

1.6 Market Damages

We implement country-specific empirical relationships, based on country deviations from the model in Burke et al. [2015]. We then build a model to explain those deviations using values from the INFORM risk index, to reflect changing vulnerability.

The current market damages estimates, which reflect the main result of Burke et al. [2015], do not allow for adaptation or differential vulnerability, which are strengths of PAGE.

Burke et al. [2015] reports country-level estimates of the marginal effect of temperature on GDP growth (see figure 5). We would like to evaluate these differences relative to indices that describe the historical vulnerability of countries. The IPCC's AR6 WGII report considered two of these indices, the INFORM Risk Index and WorldRiskIndex. We evaluate the ability of these indices and of log GDP per capita to explain the deviation. The INFORM risk estimates both explain the estimates and conform to the theory that higher-vulnerability countries should see greater marginal losses to temperature increases (see figure 6). In addition, future projected INFORM indices are available to describing future vulnerability.

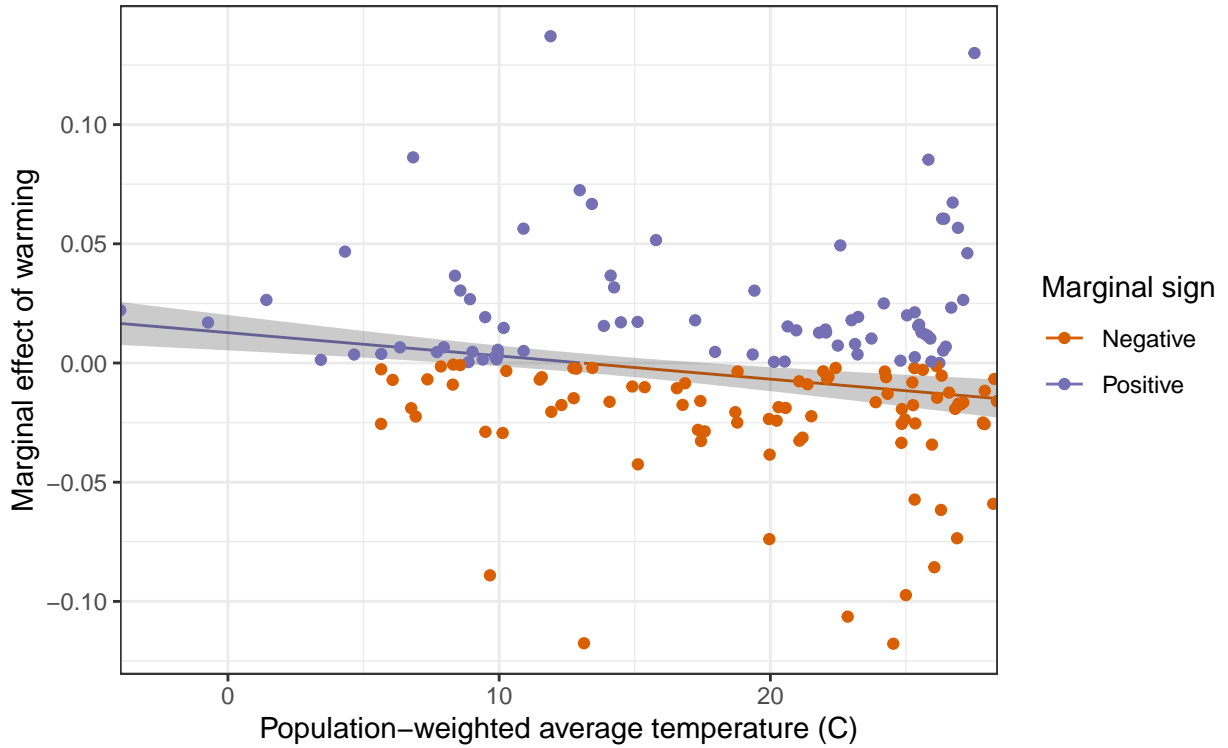


Figure 5: Country-level deviations in the marginal effect of temperature on GDP growth from the global marginal dose-response curve estimated in Burke et al. [2015].

The INFORM model provides country-level information on Hazard & Exposure, Vulnerability, and Lack of Coping Capacity. We use a Bayesian MCMC system (Stan) to estimate the relationships between these and the country-level deviations, according to

$$\Delta_i = \alpha + \beta_1 \text{Hazard \& Exposure} + \beta_2 \text{Vulnerability} + \dots \quad (5)$$

$$+ \beta_3 \text{Lack of Coping Capacity} + \gamma \text{Log GDP p.c.} + \epsilon_i \quad (6)$$

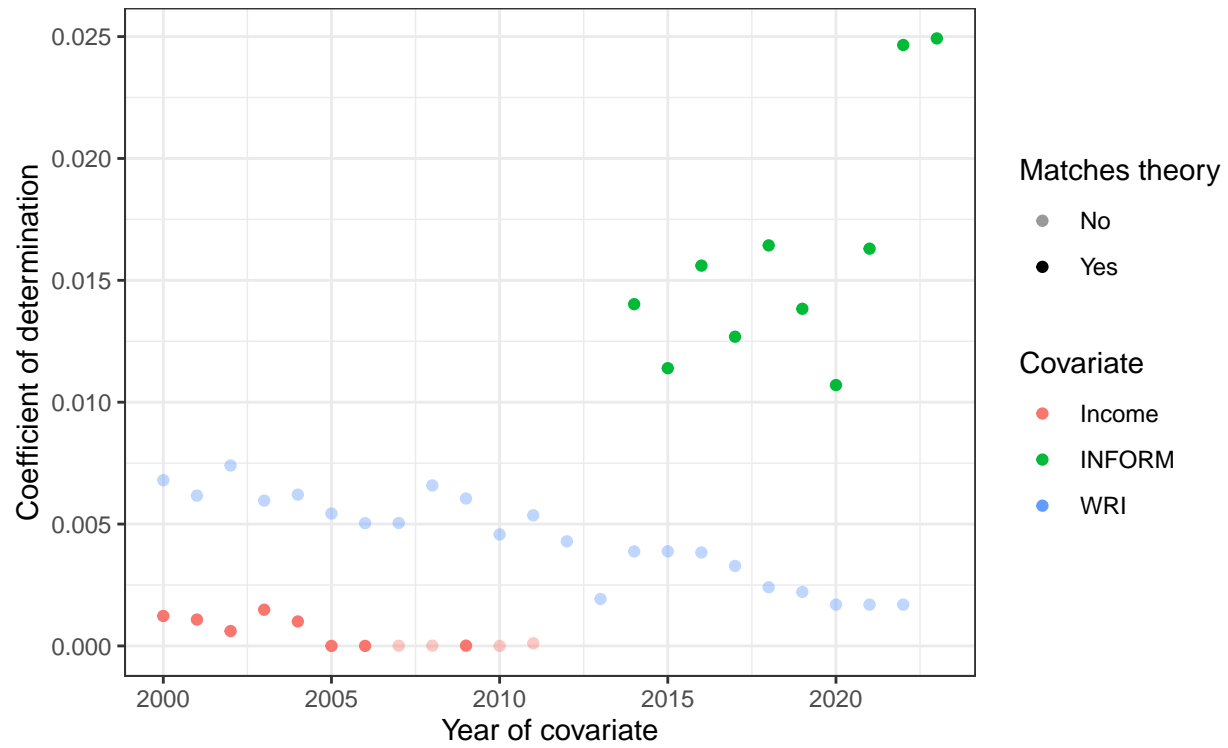


Figure 6: Evaluation of available vulnerability indices to explain country-level deviations in marginal temperature effects.

We use inverse variance weighting to account for the uncertainty in deviation estimates, and impose the constraint that $\beta < 0$ and $\gamma > 0$. The results are shown in figure 7 and the final explained deviations are shown in figure 8.

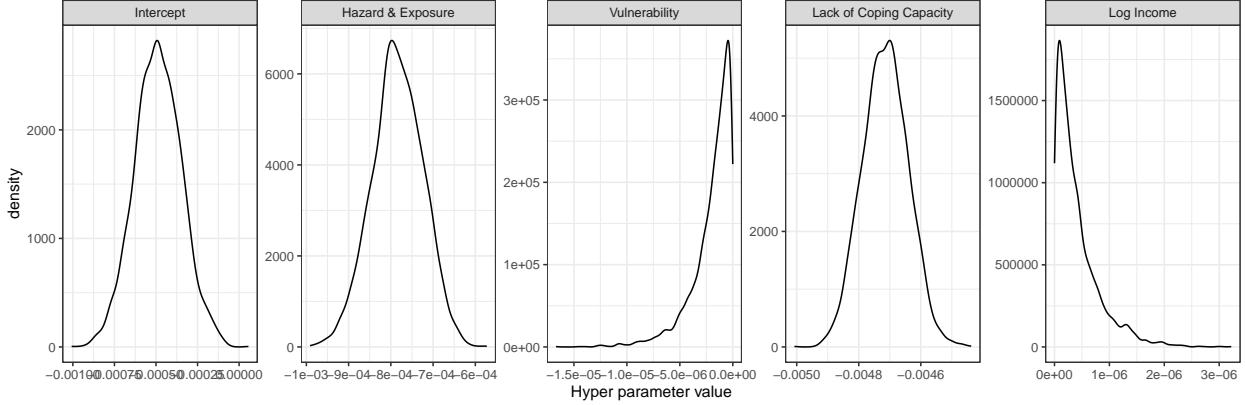


Figure 7: Marginal effects of vulnerability risk index elements to explain deviations in the marginal effect of temperatures.

1.7 Non-market damages

We derive a new estimate of non-market damages using the meta-analysis by Howard and Sterner [2017]. The approach also uses PAGE’s method of determining willingness-to-pay as a function of income levels.

The following text is modified from the supplemental information descriptions in a paper in preparation on the social cost of methane.

Market damages are those climate damages affecting economic activity mediated by money. Market damages do not include estimates of the welfare cost of climate change outside markets, for example loss of human life or damages to ecosystems that can be priced at people’s willingness to pay (WTP) to preserve those ecosystems’ existence. ‘Non-market’ damages are more uncertain than their market counterparts, but in many IAMs they occupy a substantial share of total welfare damages from climate change [e.g. Nordhaus and Boyer, 2000, Rennert et al., 2022a].

The current estimate of non-market damages in PAGE have not been recently calibrated. As part of a separate project, we have implemented non-market damages using the structure described by the MERGE IAM [Manne and Richels, 2005], with an updated calibration derived from Howard and Sterner [2017]. The MERGE model places particular emphasis on the representation of non-market damages, with a WTP measure that depends on both income and temperature. While the parameters of the MERGE non-market damage module are speculative, its use of an S-shaped elasticity of WTP with respect to income is theoretically coherent.

Like the MERGE model, the damage function meta-analysis by Howard and Sterner [2017] assumes that damages grow quadratically with warming from a pre-industrial baseline. Under their preferred model, total damages as a percent of GDP (including market and non-market impacts) follow $0.595\Delta T_{AT}(t)^2$. Considering only damage functions that exclude non-market damages, their key coefficient is reduced by 0.487.¹ We use this as evidence that non-market damages follow $0.487\Delta T_{AT}(t)^2$. As in Howard and Sterner [2017], we increase this coefficient by 25%, to 0.609, to account for potential omitted (non-catastrophic) damages. This

¹This coefficient comes from table 2, column 3 of Howard and Sterner [2017]. While their preferred model is column 4, that model has a market-only reduction of 0.622, larger than the total damage coefficient. Columns 3 and 4 estimate identical values for the total damage coefficient, so we use the more conservative value.

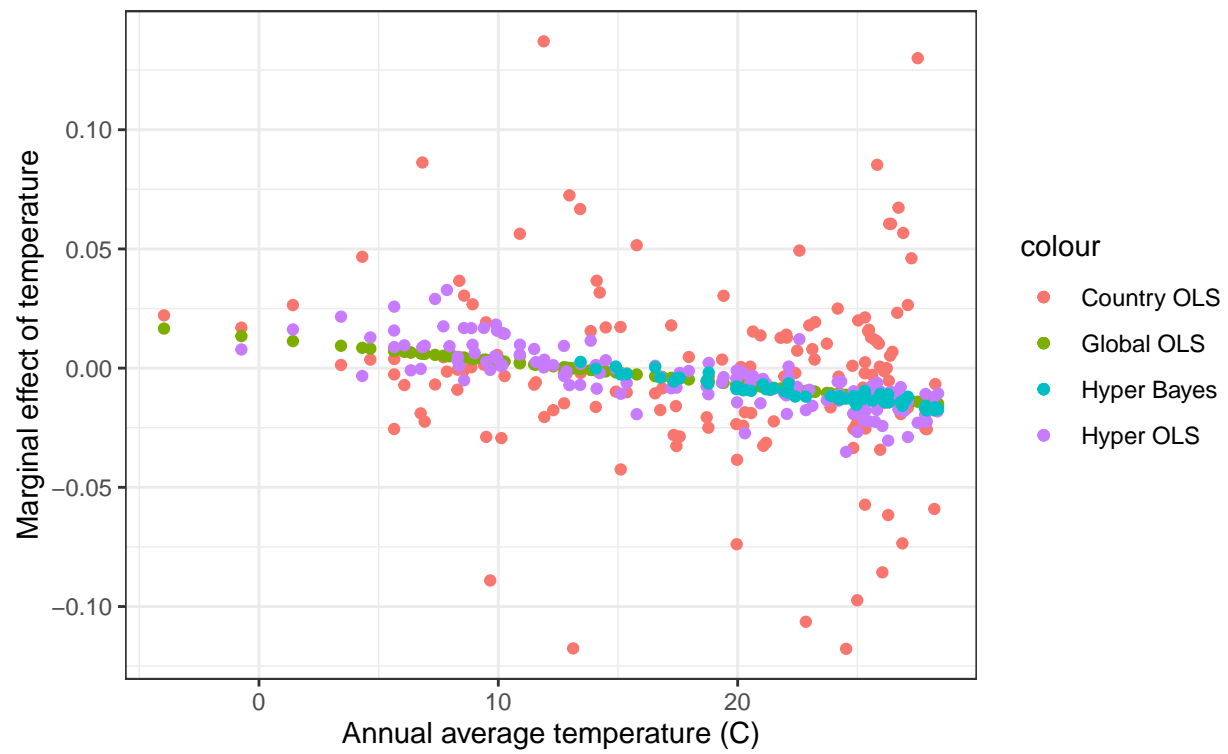


Figure 8: Country-level marginal effects, as explained by the available risk index components.

COUNTRY	Baseline (current) risk (B)	MID-CENTURY (~2050) CRISIS RISK						END-CENTURY (~2080) CRISIS RISK					
		PESSIMISTIC (P) climate and socio-economic scenario			OPTIMISTIC (O) climate and socio-economic scenario			PESSIMISTIC (P) climate and socio-economic scenario			OPTIMISTIC (O) climate and socio-economic scenario		
		INFORM Climate Change (CC) Risk Index 2022	INFORM CC Risk Index	Change in risk	Vulnerability gap	INFORM CC Risk Index	Change in risk	Vulnerability gap	INFORM CC Risk Index	Change in risk	Vulnerability gap	INFORM CC Risk Index	Change in risk
Kenya	4.6	5.1	0.5	1.0	4.8	0.2	0.4	5.3	0.7	1.4	4.8	0.2	0.5
Kiribati	3.0	3.7	0.7	1.5	3.7	0.7	1.5	3.7	0.7	1.6	3.7	0.7	1.5
Korea DPR	4.6	4.7	0.1	0.3	4.6	0.0	0.1	4.8	0.2	0.4	4.6	0.0	0.1
Korea Republic of	2.1	2.1	0.0	0.0	2.1	0.0	0.0	2.0	-0.1	-0.0	2.1	0.0	0.0
Kuwait	1.7	2.2	0.5	0.4	2.2	0.5	0.3	2.3	0.6	0.4	2.2	0.5	0.3
Kyrgyzstan	2.7	2.8	0.1	0.1	2.7	0.0	0.1	2.9	0.2	0.3	2.7	0.0	0.1
Lao PDR	4.0	4.0	0.0	-0.1	3.9	-0.1	-0.3	4.0	0.0	0.0	3.9	-0.1	-0.3
Latvia	1.3	1.4	0.1	0.1	1.4	0.1	0.1	1.6	0.3	0.2	1.5	0.2	0.1
Lebanon	3.9	4.2	0.3	0.5	4.0	0.1	0.1	4.3	0.4	0.7	4.1	0.2	0.2
Lesotho	3.0	3.7	0.7	2.1	3.5	0.5	1.7	3.9	0.9	2.5	3.6	0.6	1.9

Figure 9: Excerpt from the INFORM Climate Change Oct. 2022 report.

gives a 90% increase in WTP relative to Manne and Richels [2005]. At 2.5°C warming, WTP is 3.8% of GDP, compared to 2.0% in the original MERGE calibration (see Figure 10).

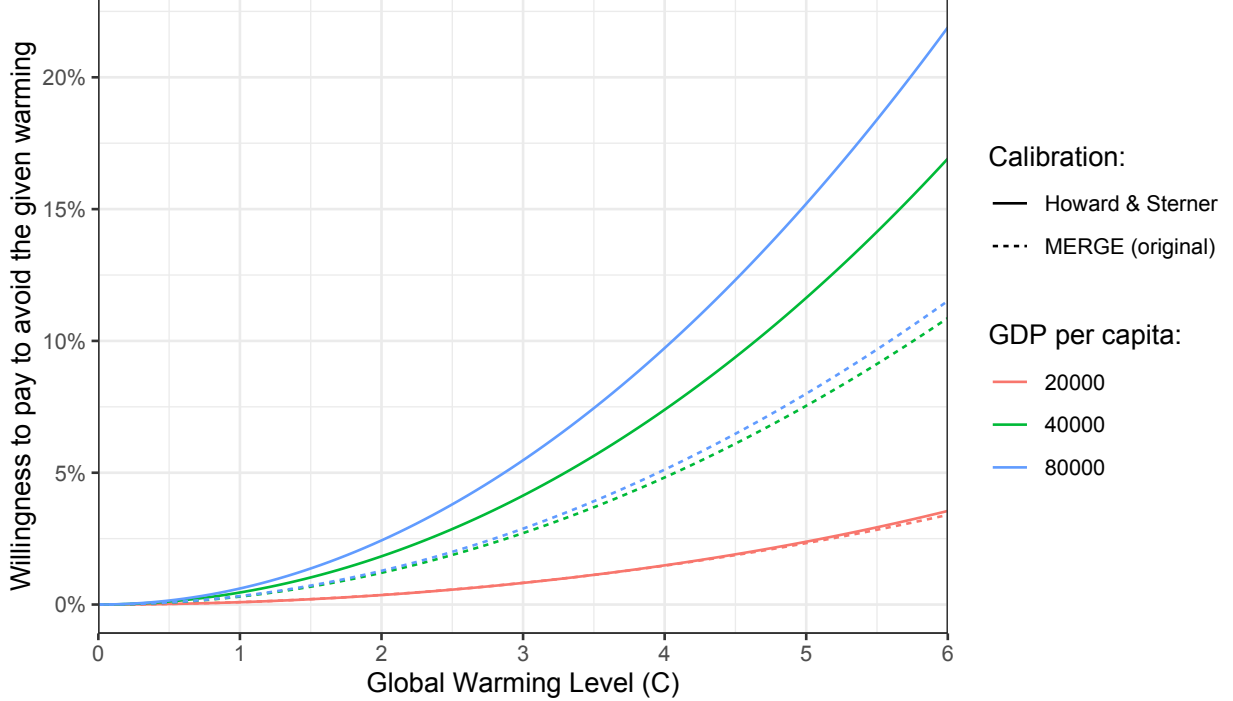


Figure 10: Willingness to pay to avoid levels of warming, split by levels of income. The original and updated calibrations are shown.

This WTP applies at high incomes. MERGE provides a model to link WTP to income, which we maintain. At \$25k/capita, WTP to avoid 2.5°C warming is held at 1%. As income increases above that level, WTP asymptotically approaches the non-market damages from Howard and Sterner [2017]. WTP to avoid warming as a function of income is shown in Figure 11.

We calculate this WTP measure at a national level. The non-market damage multiplier, or economic loss function, is

$$D_{\text{NM}}(i, t) = \left[1 - \left(\left(\frac{\Delta \overline{T}_{\text{AT}}(t)}{\Delta T_{\text{cat}}} \right)^2 - \left(\frac{\Delta \overline{T}_{\text{AT}}(0)}{\Delta T_{\text{cat}}} \right)^2 \right) \right]^{h(i, t)}. \quad (7)$$

where $\overline{T}_{\text{AT}}(0)$ is the temperature in the baseline period, which is taken to be 2010.

This is a hockey-stick function embodying the assumption that non-market damages can increase rapidly as temperatures become more extreme. ΔT_{cat} is a catastrophic warming parameter set to 12.82°C , which people are assumed to be willing to avoid at any cost². $h(i, t)$ is the hockey-stick parameter, which depends on country income per capita ($y(i, t)$):

$$h(i, t) = \min \left[\frac{\log \left[1 - \frac{D_{\text{ref}}}{1 + 100 \exp[-WTP_{\text{ref}}y(i, t)]} \right]}{\log \left[1 - (\Delta T_{\text{ref}}/\Delta T_{\text{cat}})^2 \right]}, 1 \right], \quad (8)$$

²The catastrophic warming temperature is derived from the assumption that economic losses rise quadratically according to the Howard and Sterner [2017] calibration.

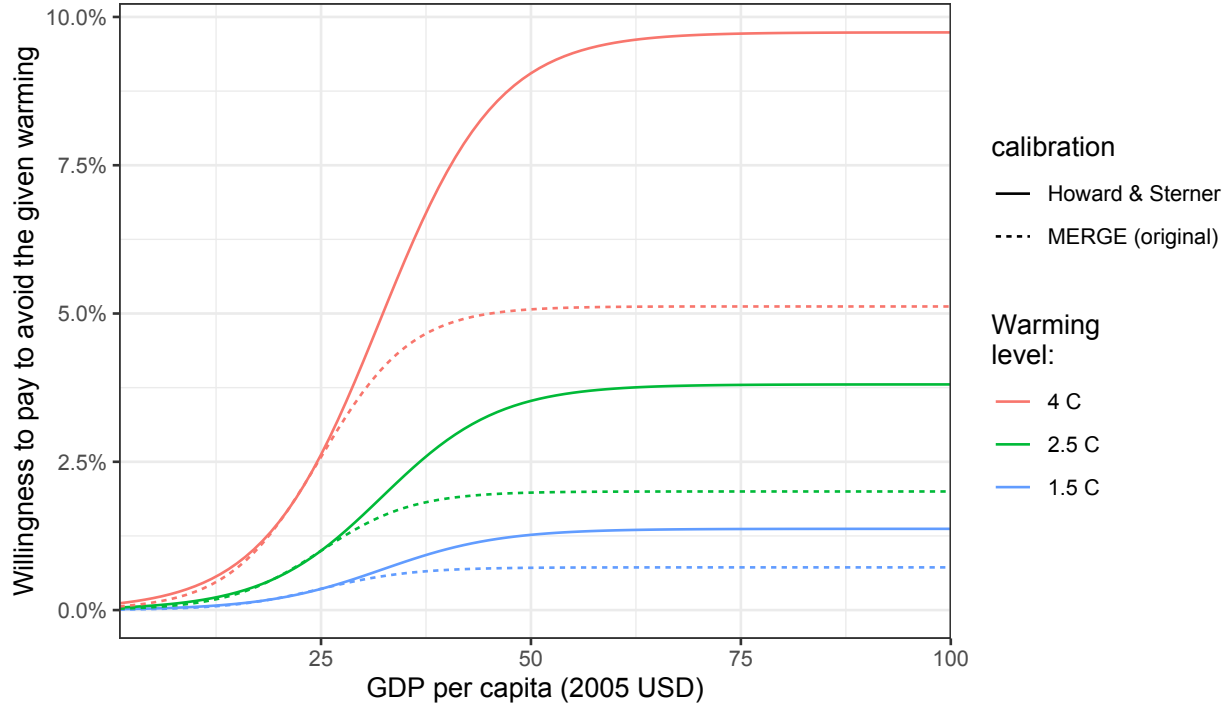


Figure 11: Willingness to pay to avoid 1.5, 2.5, and 4 °C, as a function of income, under the original and updated calibrations.

where

$$\begin{aligned}
 WTP_{ref} &= 0.143 && \text{WTP 1\% of GDP to avoid reference warming at \$25k/capita} \\
 D_{ref} &= 0.038 && \text{WTP loss at reference warming} \\
 \Delta T_{ref} &= 2.5 \text{ C} && \text{WTP reference warming}
 \end{aligned}$$

1.8 Sea-level rise damages

The following text is modified from the supplemental information descriptions in a paper in preparation on climate damages in the United Kingdom.

The Coastal Impact and Adaptation Model (CIAM) has been built to study the impacts of sea level rise on coastlines worldwide, under different assumptions about adaptation that include the possibility of optimal (least-cost) adaptation planning. The model was introduced and is described in detail in Diaz [2016]. The data and implementation that we rely upon here is drawn from Depsky et al. [2023], updated as part of the Climate Impact Lab's Social Cost of Carbon work.

CIAM works at a high spatial resolution by building on the Dynamic Interactive Vulnerability Assessment (DIVA) database [Hinkel and Klein, 2009]. DIVA partitions the world's coastlines into 12 148 segments with homogeneous physical characteristics. The median length of a segment is 18km. South Korea's coastline, for example, is divided into 105 segments. Cost estimates at the segment level can be aggregated to coarser spatial scales, for example the country and global levels. CIAM runs in time steps of 10 years. It is initialised in the year 2000 and can run up to 2200, though we mainly focus on the period up to 2100. The base year currency is 2010 US dollars.

Each segment in CIAM is described by its physical attributes (coastline length, surface area by elevation, storm surge frequency, wetland extent), socio-economic attributes (income, population density, capital stock), as well as protection costs. Physical attributes are taken from DIVA, while socio-economic attributes and protection costs are derived from a range of sources described in Diaz [2016]. While some segment attributes such as length are time-invariant, most are time-varying. Future segment population is based on the United Nations' projections, while future segment income is based on IMF projections.

There are five categories of coastal impact in CIAM:

- Protection costs (construction of sea walls, dikes, etc.);
- Retreat costs (relocating people and mobile capital inland, and demolishing immobile capital);
- Inundation costs (the value of lost land, and immobile capital abandoned);
- Wetland costs (the value of lost wetland ecosystem services);
- Flood costs (expected damage to capital stocks and expected mortality from storm surges).

The overall cost of sea level rise is the sum of each of these five cost categories, the first two of which can be regarded as adaptation costs, while the latter three can be regarded as residual damages.

Both overall costs and their composition depends on what is assumed about adaptation. In general, each segment possesses a social planner who solves the following optimisation problem for his/her own segment:

$$\text{OverallCost} = \min_s \sum_{t \in \Delta_t} \left[\frac{1}{(1+r)^t} (\text{ProtectionCost}_{st} + \text{RetreatCost}_{st} + \text{InundationCost}_{st} + \text{WetlandCost}_{st} + \text{FloodCost}_{st}) \right]$$

where s is the adaptation strategy, Δ_t is the adaptation planning period comprising decadal time-steps t , and r is the discount rate.

When the adaptation strategy s corresponds to no adaptation, $\text{ProtectionCost}_t = 0$ for all t and RetreatCost_t is optimally chosen to react to sea level rise at the same time step. Alternatively, when s corresponds to optimal adaptation, both ProtectionCost and RetreatCost are chosen once during each adaptation planning period in order to minimise the discounted OverallCost of sea level rise in the current and next adaptation planning periods.

This problem is solved independently for each of CIAM's 12 148 segments and sequentially for each adaptation planning period. Thus, when adapting optimally the planner looks forward one period in each planning period. Perfect foresight is assumed, which is unrealistic but necessary for computational tractability given so many optimisation problems are being solved simultaneously. The default adaptation planning periods are 40 years, with shorter initial and final periods, i.e.: 2000; 2010-2040; 2050-2090; 2100-2140; 2150-2180; 2190-2200.

Unadapted and optimal adaptation results are shown in figure 12.

1.9 Abatement costs

Updated abatement costs estimates rely upon a country-level downscaling of abatement scenarios developed by the Network for Greening the Financial System (NGFS). These use results from GCAM, MESSAGE-GLOBIOM and REMIND-MAgPIE. We use all available scenarios under Phase 3 of that project (<https://data.ece.iiasa.ac.at/ngfs-phase-3/>).

Two emulators are developed using this data, to describe (1) how emissions are reduced as a function of carbon price, and (2) how GDP is reduced as a function of carbon price. We estimate a piece-wise linear curve, constrained so that higher carbon prices produce both higher mitigation and higher costs. We also assume that these relationships change over time. The emulator regressions are:

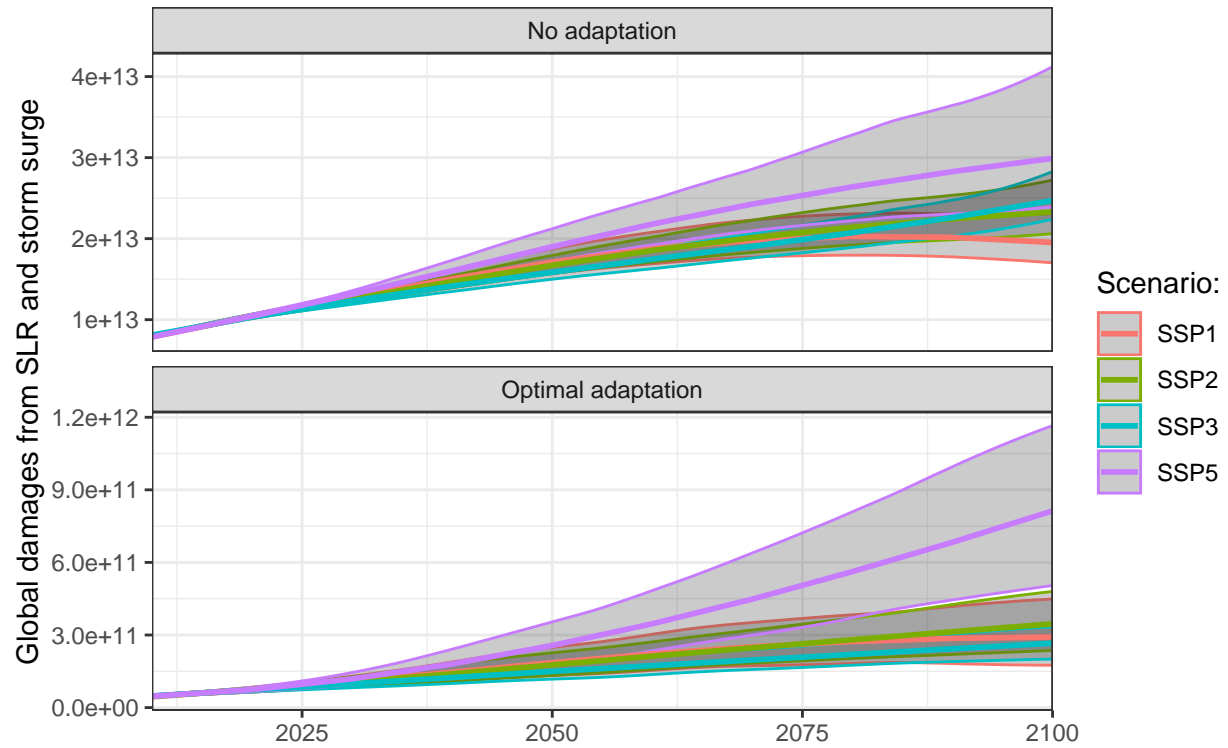


Figure 12: Global damages from sea-level rise and storm surge, according to the model by Depsky et al. [2023].

$$\text{Emit}_i = \sum_k \alpha_k S_k(p_i) + \sum_k \beta_k S_k(p_i)(t_i - 2000) + \gamma \text{LagEmit}_i + \delta_{t_i} + \eta_{m_i} \quad (9)$$

$$\text{LogGDP}_i = \sum_k \alpha_k S_k(p_i) + \sum_k \beta_k S_k(p_i)(2050 - t_i) + \gamma \text{LagLogGDP}_i + \delta_{t_i} + \eta_{m_i} \quad (10)$$

$$(11)$$

such that $\alpha_k < 0, \beta_k < 0, \gamma > 0, \delta_t > 0, \eta_m > 0$.

Finally, we impose a regularization on the resulting mitigation relationships, so that total abatement asymptotically approaches 100%. This is

$$\text{RawFractionAbated}/(\exp(-\text{CarbonPriceUSD}/500) + \text{RawFractionAbated}) \quad (12)$$

The resulting regularized mitigation curves are shown in figure 13.

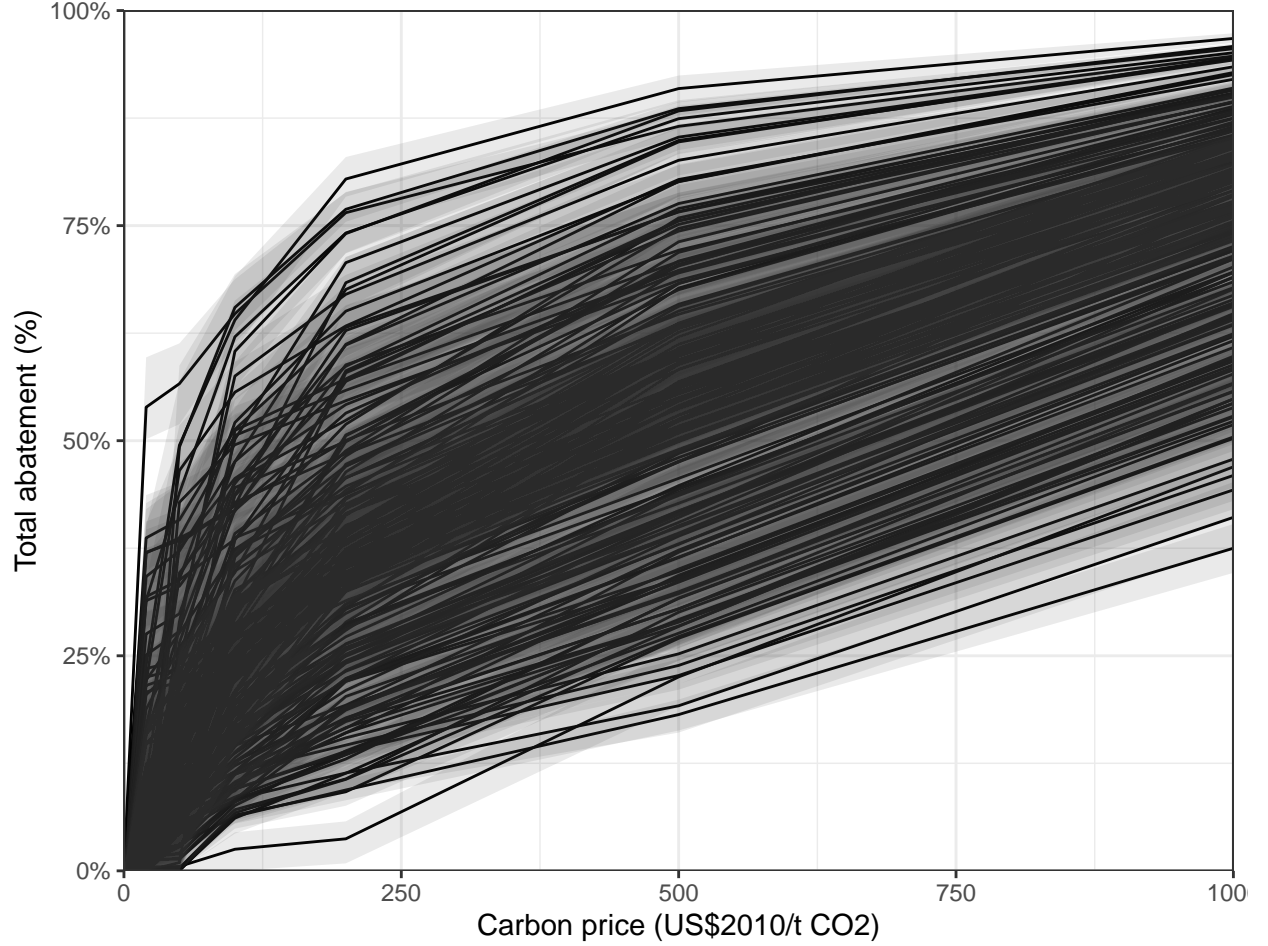
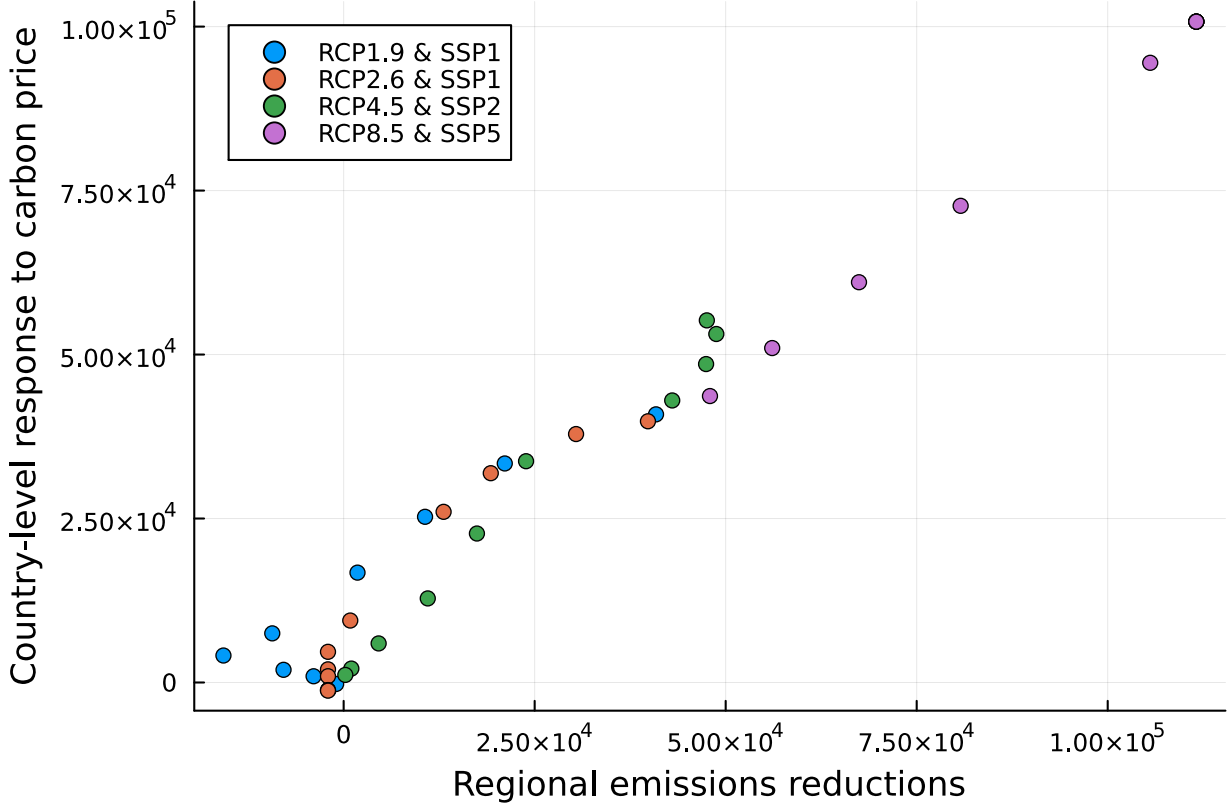


Figure 13: Portion of emissions mitigated for each country (shown as a separate line) as a function of the carbon price.

These estimates only apply to CO₂ mitigation, while PAGE has mitigation cost estimates for each gas. Other cost estimates will continue to be computed at a regional level.



1.10 Downscaling of CO₂ and CH₄

Country-level CO₂ and CH₄ emissions are based on emission estimates for the year 2015, with emissions growth rates used in PAGE-ICE.

1.11 Subnational damages

While national units are appropriate for many applications, including mitigation policy and loss & damage remuneration, they are still coarse relative to the heterogeneity in damages [Hsiang et al., 2017, Carleton et al., 2022]. In this section, we provide a mechanism for adjusting national damages taking into account subnational damage distributions.

Subnational heterogeneity in damages can produce changes in welfare-equivalent damages and the SCCO₂ under equity-weighting assumptions [Anthoff et al., 2009]. Since the damages are calibrated to reflect national totals, these and the associated SCCO₂ values are correct in the absence of equity-weighting. However, since standard utility functions are concave, equity-weighting is a direct consequence of standard welfare economic theory.

We start by assuming that subnational incomes are log-normally distributed, and use Gini coefficients from the INFORM Risk 2023 dataset to calibrate these distributions, so that the income for individual i from country j is described as

$$\log y_{ji} \sim \mathcal{N}(\bar{y}_j - \sigma_j^2/2, \sigma_j^2)$$

where $\sigma_j = \sqrt{2}\phi^{-1}(Gini_j/100 + 1/2)$.

We also define a vulnerability coefficient, v_{ji} , also log-normally distributed. Damages for individual i are

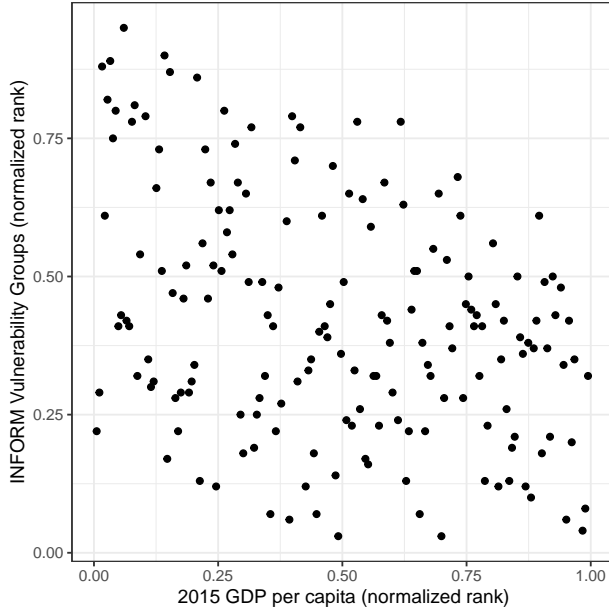
defined as the country-level damages, times vulnerability, and v_{ij} is centered at 1:

$$\log v_{ji} \sim \mathcal{N}(-\tau_j^2/2, \tau_j^2)$$

where τ_j is defined as the INFORM Risk 2023's index of vulnerable groups divided by 10. The vulnerable groups index is from 0 to 10, so the 99th percentile of vulnerability is 10 times the country-level average.

Finally, for either the vulnerability or income distributions to affect total damages, a correlation must exist between these two variables (e.g., lower-income individuals may be more likely to have higher vulnerability). We find that the correlation between income rank and vulnerability rank, as reported at the country level in INFORM Risk 2023, is -0.36 . We bootstrap this estimate across countries to generate the distribution of correlations in figure 14 (b), and define $\log y_{ji}$ and $\log v_{ji}$ as a multivariate normal with a correlation drawn from this distribution.

(a) Rank of income vs. vulnerability



(b) Bootstrapped correlation between income and vulnerability

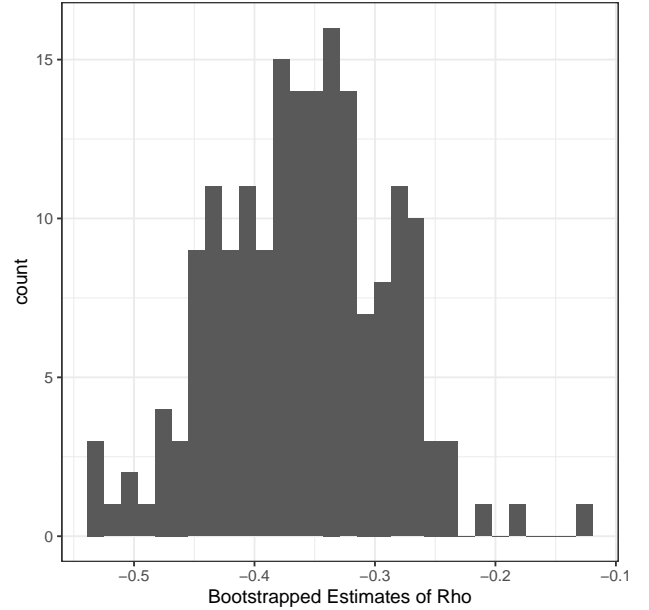
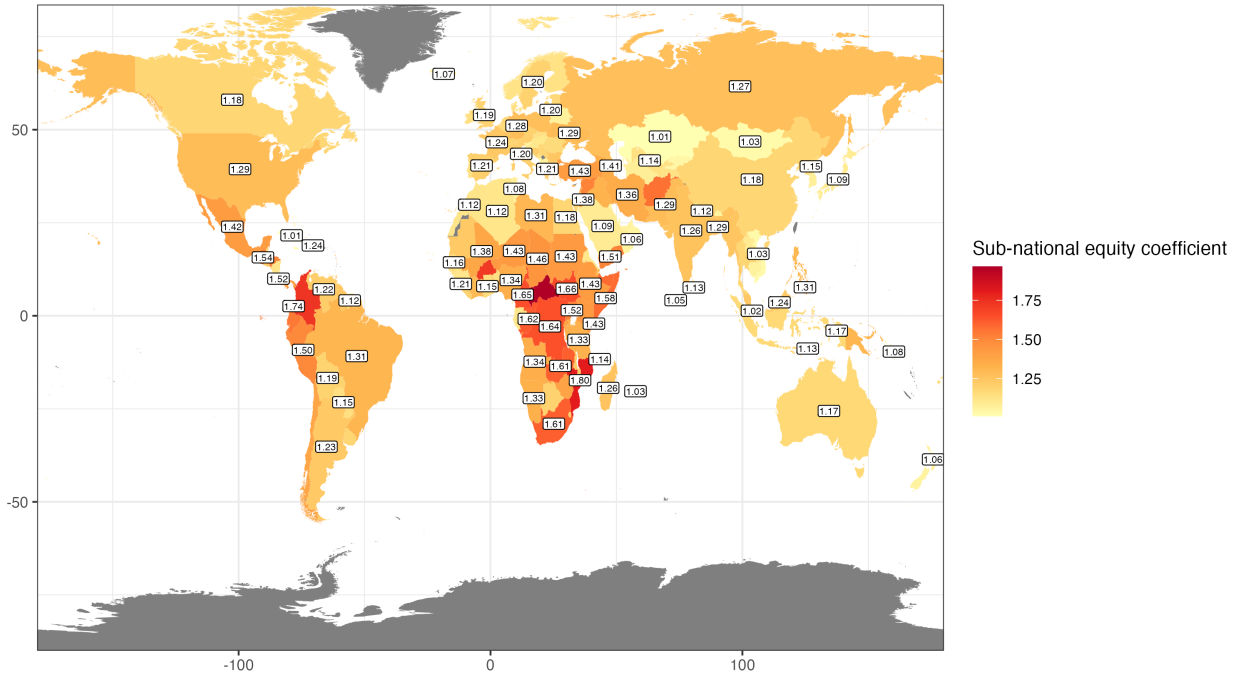


Figure 14: Estimation of the rank correlation between baseline income (2015 USD) and vulnerability (scores from INFORM Risk 2023).

Under power utility, the SCCO₂ under these subnational distributions is

$$\begin{aligned} \frac{dW/de}{\partial W/\partial y} &= \frac{\frac{d}{de} \int_v \int_y p_{vy} vu(y) dy dv}{\frac{\partial}{\partial y} \int_v \int_y p_{vy} u(y) dy dv} \\ &= \frac{\sum_i v_i \frac{d}{de} u(y)}{\sum_i \frac{\partial}{\partial y} u(y)} \\ &= \frac{1}{N} \sum_i v_i \left(\frac{y}{\bar{y}}\right)^{1-\eta} \text{SCCO}_2 \end{aligned}$$

We calculate $\frac{1}{N} \sum_i v_i \left(\frac{y}{\bar{y}}\right)^{1-\eta}$ for each country. These are shown in the figure below:



2 Model Availability

The model is available on Github at <https://github.com/openmodels/MimiPAGE2025.jl/>.

.1 Expert Elicitation Discounting

Drupp et al. [2018] provide values for the pure rate of time preference (PRTP) and the elasticity of marginal substitutability from 181 experts. The median of these values is a PRTP of 0.5% and an elasticity of 1, and we use these values for a central preference estimate. When we provide a range across preference parameters, we draw paired PRTP and elasticity values from the dataset, to maintain any dependence between them. These values are summarized in figure 15.

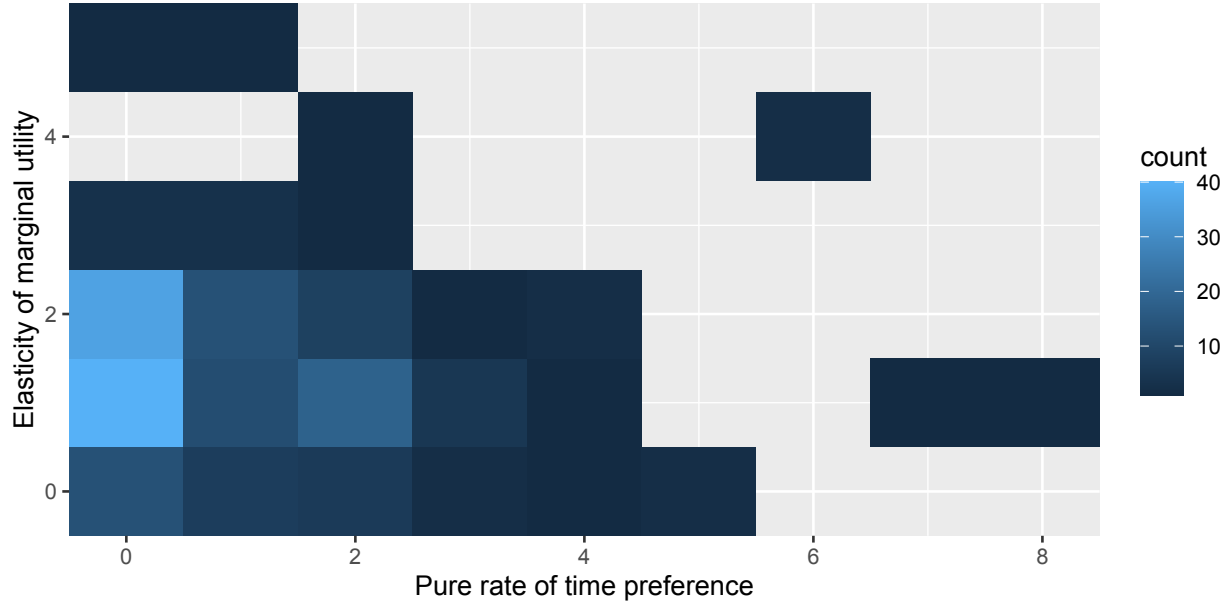


Figure 15: Caption

References

- D. Anthoff, C. Hepburn, and R. S. Tol. Equity weighting and the marginal damage costs of climate change. *Ecological Economics*, 68(3):836–849, 2009.
- M. Burke, S. M. Hsiang, and E. Miguel. Global non-linear effect of temperature on economic production. *Nature*, 527(7577):235–239, 2015.
- T. Carleton, A. Jina, M. Delgado, M. Greenstone, T. Houser, S. Hsiang, A. Hultgren, R. E. Kopp, K. E. McCusker, I. Nath, et al. Valuing the global mortality consequences of climate change accounting for adaptation costs and benefits. *The Quarterly Journal of Economics*, 137(4):2037–2105, 2022.
- N. Depsky, I. Bolliger, D. Allen, J. H. Choi, M. Delgado, M. Greenstone, A. Hamidi, T. Houser, R. E. Kopp, and S. Hsiang. Dscim-coastal v1. 1: an open-source modeling platform for global impacts of sea level rise. *Geoscientific Model Development*, 16(14):4331–4366, 2023.
- D. B. Diaz. Estimating global damages from sea level rise with the coastal impact and adaptation model (ciam). *Climatic Change*, 137(1):143–156, 2016.
- S. Dietz, J. Rising, T. Stoerk, and G. Wagner. Economic impacts of tipping points in the climate system. *Proceedings of the National Academy of Sciences*, 118(34):e2103081118, 2021.
- M. A. Drupp, M. C. Freeman, B. Groom, and F. Nesje. Discounting disentangled. *American Economic Journal: Economic Policy*, 10(4):109–134, 2018.
- S. E. Fick and R. J. Hijmans. Worldclim 2: new 1-km spatial resolution climate surfaces for global land areas. *International journal of climatology*, 37(12):4302–4315, 2017.
- J. Hinkel and R. J. Klein. Integrating knowledge to assess coastal vulnerability to sea-level rise: The development of the diva tool. *Global Environmental Change*, 19(3):384–395, 2009.
- P. H. Howard and T. Sterner. Few and not so far between: a meta-analysis of climate damage estimates. *Environmental and Resource Economics*, 68(1):197–225, 2017.

- S. Hsiang, R. Kopp, A. Jina, J. Rising, M. Delgado, S. Mohan, D. J. Rasmussen, R. Muir-Wood, P. Wilson, M. Oppenheimer, et al. Estimating economic damage from climate change in the united states. *Science*, 356(6345):1362–1369, 2017.
- J. S. Kikstra, P. Waidelich, J. Rising, D. Yumashev, C. Hope, and C. M. Brierley. The social cost of carbon dioxide under climate-economy feedbacks and temperature variability. *Environmental Research Letters*, 16(9):094037, 2021.
- A. S. Manne and R. G. Richels. Merge: an integrated assessment model for global climate change. In *Energy and environment*, pages 175–189. Springer, 2005.
- W. D. Nordhaus and J. Boyer. *Warming the World: Economic Models of Global Warming*. MIT Press (MA), 2000.
- D. Rasmussen, M. Meinshausen, and R. E. Kopp. Probability-weighted ensembles of us county-level climate projections for climate risk analysis. *Journal of Applied Meteorology and Climatology*, 55(10):2301–2322, 2016.
- K. Rennert, F. Errickson, B. C. Prest, L. Rennels, R. G. Newell, W. Pizer, C. Kingdon, J. Wingenroth, R. Cooke, B. Parthum, et al. Comprehensive evidence implies a higher social cost of co2. *Nature*, 610 (7933):687–692, 2022a.
- K. Rennert, B. C. Prest, W. A. Pizer, R. G. Newell, D. Anthoff, C. Kingdon, L. Rennels, R. Cooke, A. E. Raftery, H. Ševčíková, et al. The social cost of carbon: advances in long-term probabilistic projections of population, gdp, emissions, and discount rates. *Brookings Papers on Economic Activity*, 2021(2):223–305, 2022b.